VALENCE CHARGE MAPPING AND POTENTIAL TRAP DEPRESSION IN GRAPHENE MEMBRANES AND CARBON NANOTUBES

Luca Ortolani[1], Florent Houdellier[2], Etienne Snoeck[2], Marc Monthioux[2] and Vittorio Morandi[1]

[1] CNR IMM-Bologna, Via Gobetti 101, 40129 Bologna (Italy), [2] CNRS CEMES, 29 Rue Jeanne Marvig, 31055 Toulouse (France)

Introduction

The band structure of graphene presents six conical points where the energy dispersion is perfectly linear in the momentum. This particular feature is at the basis of the interesting physical and chemical properties of this material [1]. Unfortunately, upon stacking to form a Few-Graphene-Crystal (FGC), the weak interlayer interaction could induce a small valence charge redistribution in the crystal lattice, suppressing the linear dispersion in the band-structure [2]. In particular, in turbostratic FGCs, the interlayer charge redistribution, and hence the electronic structure of the crystal, depend on the rotation angle between the graphenes [3]. For certain orientations, when the lattices are commensurable, graphenes electronically decouple, and the FGC behaves like an individual monolayer [4]. Using transmission electron holography [5], we investigated the redistribution of electronic crystal charges in a turbostratic FGC, in which the number of layers varies from an individual graphene up to four. Using the same technique we probed the charge distribution in individual carbon nanotubes (CNTs), investigating charge redistributions as the number of walls (= graphenes) decreases from 20 (concentric multi-walled (MW-) CNTs) down to a single-wall (SW-) CNT.

Experimental

Turbostratic FGCs were prepared by means of a liquid assisted mechanical exfoliation of natural Madagascar graphite powder, as recently proposed [6]. MWCNTs and SWNTs grown by arc-discharge were dispersed in acetone with the aid of sonication. TEM samples were prepared by simple drop-casting onto standard holey-carbon-film grids for transmission electron microscopy (TEM) investigation. TEM characterization was performed using a Tecnai F20 microscope, equipped with a CEOS aberration corrector and an electrostatic biprism. A customized electro-optical set-up was developed to allow the microscope to be operated at an accelerating voltage of 100kV to reduce beam damage to the sample. Phase reconstruction was done using HoloJ software [7].

Results and Discussion

Electron holography is an experimental technique capable of retrieving the full electronic wavefront of the electronic radiation that has interacted with the sample [5]. The electronic wave, passing through the specimen in the TEM, interacts with the distribution of charges in the crystal, and a detailed map of the distribution of the electric and magnetic fields is stored in the phase term of the retrieved wavefront [8]. In the absence of either magnetic contributions or free charges in the material, as in the case of FGC membranes, the measured electronic phase map $\varphi(r)$ is simply related to the electrostatic potential V in the sample, via [8]:

$$(1) \quad \varphi(r) = C_E \int V(r,z)\, dz$$

where C_E is an interaction constant depending on the energy of the beam electrons. The result of the integration in Equation (1) is the projection along the z-axis of the electrostatic potential generated by the charge distribution in the crystal.

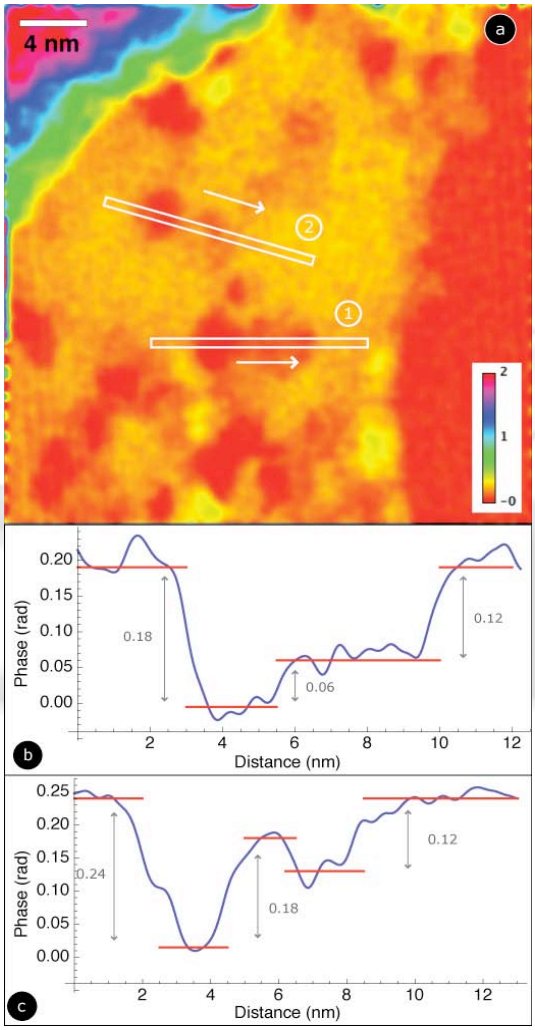

Fig. 1 Reconstructed phase map of the turbostratic graphene membrane. a) Phase map in false colors. Red corresponds to vacuum values, showing the presence of holes over the surface of the flake. b) and (c) show the phase profile along the lines indicated by (1) and (2) in the phase map.

Fig. 1a shows the reconstructed phase map, in false colors, of a turbostratic FGC composed of four graphenes. Using high-resolution (HR-) TEM imaging we determined the lattice orientation in each graphene composing the crystal. Each crystal plane was rotated by 13° with respect to its neighbors, corresponding to a commensurate turbostratic stacking [4]. The

red regions in Fig. 1a, in which the phase has the same value as in vacuum, reveal the presence of holes over the surface of the flake. Fig. 1b shows the phase profile acquired from the region indicated by (1), while Fig. 1c shows the phase profile from region (2). Nearby the holes the flake is thinner, as more graphene layers are peeled off from the crystal by electron beam damaging. The graphs clearly display step-like phase profiles, ranging from values close to zero in correspondence to vacuum, up to 0.24 rad, where four graphenes are stacked. In particular, in Fig. 1b a phase level of 0.06 rad is clearly visible, while all the other phase values correspond to multiple integers, up to four times, of this amount.

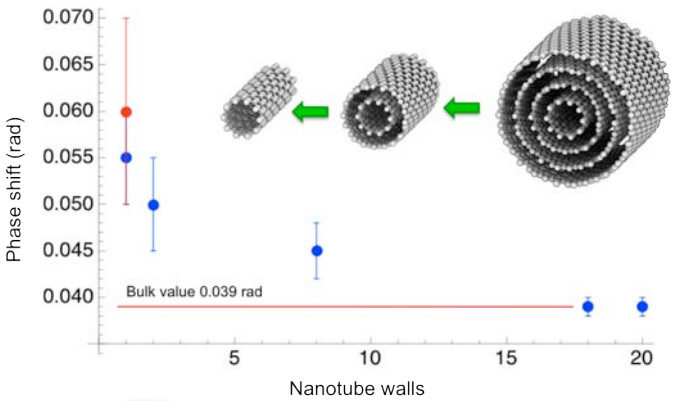

Fig. 2 Plot of the measured phase shift per graphene *versus* the number of stacked graphenes in graphene systems with turbostratic structure. Blue: in CNTs, from a 20-wall MWCNT to a SWCNT. Red: for an individual (flat) graphene, either single or within a stack with commensurable structure.

We also measured the phase shift induced by different MWCNTs, for which the stacking cannot be otherwise than turbostratic and non commensurate, with the number of walls from 20 down to a SWCNT. For each tube we calculated the average phase shift induced by each wall (i.e. the phase of an individual curved graphene). Fig. 2 shows the graph of the average phase shift per wall as experimentally determined in the case of the CNTs and the measured value for individual graphene. We notice an interesting surface effect which is not seen in the case of the FGC of Fig. 1, i.e., the phase shift increases as the number of walls decreases. This effect on the phase is not specific to carbon nanotubes. It has also been predicted and experimentally confirmed for gold nanoparticles [9], for which it has been attributed to the redistribution of valence charges in the under-coordinated atoms of the surface. A similar effect has been predicted for CNTs [10]. When the number of walls in the tube is large (more than ~15), the surface effect on the average phase shift is screened by the bulk contribution of the inner graphenes, bonded by weak van der Waals forces. In this configuration, the phase shift per graphene is close to 0.04 rad, i.e., the same value as expected and measured for bulk graphite [11]. In the case of the FGC of Fig. 1, the commensurability between graphene lattices makes each graphene to be electronically decoupled from its neighbors [3]. This makes each graphene within the stack shift the electron beam as an individual graphene, behaving similarly to a surface graphene.

Conclusions

We used transmission electron holography to probe crystallographic charge redistributions in turbostratic FGCs and CNTs, as the number of graphenes varies. For the first time to our knowledge, we measured the phase shift induced by an individual single-atom-thin graphene, and mapped the phase shift variation throughout a whole FGC in relation with the local number of graphenes. On the other hand, the phase investigation of the turbostratic, non commensurate stacking of graphenes in concentric MWCNTs revealed a size effect originating from the charge redistribution in the under-coordinated surface graphene. The data shows an increase of the phase shift, hence a depression of the average atomic potential traps, as the proportion of surface atoms over the total number of atoms for an individual nanotube decreases. Comparing electron phase shifts of a FGC and CNTs, we found that the commensurate stacking geometry makes each graphene in the FGC be decoupled from any neighboring graphene and shift the electron phase as a surface (or an individual) graphene does. In a non commensurate stacking (and probably ABAB stacking as well), only the actual surface graphenes of the stack shift the phase differently from inner ones.

References

[1] Neto A.H.C., Guinea F., Peres N.M.R., Novoselov K.S., Geim A. K. The electronic properties of graphene. Rev. Mod. Phys. 2009;81:109-162.
[2] Partoens B., Peeters F.M. From graphene to graphite: Electronic structure around the K point. Phys. Rev. B 2006;74:075404.
[3] Latil S., Meunier V., Henrard L. Massless fermions in multilayer graphitic systems with misoriented layers: Ab initio calculations and experimental fingerprints. Phys. Rev. B 2007;76:201402.
[4] Dos Santos J.M.B.L., Peres N.M.R., Castro Neto A.H. Graphene bilayer with a twist: Electronic structure. Phys. Rev. Lett. 2007;99:256802.
[5] Lichte H., Formanek P., Lenk A., Linck M., Matzeck C., Lehmann M., Simon P. Electron holography: Applications to materials questions. Ann. Rev. Mat. Res. 2007;37:539-588.
[6] Hernandez Y., Nicolosi V., Lotya M., Blighe F.M., Sun Z., De S., Mcgovern I.T., Holland B., Byrne M., Gun'Ko Y.K., Boland J.J. Niraj, P. Duesberg, G., Krishnamurthy S., Goodhue R., Hutchison J., Scardaci V., Ferrari A.C., Coleman J.N. High-yield production of graphene by liquid-phase exfoliation of graphite. Nat. Nanotechnol. 2008;3:563-568.
[7] Ortolani, L.; Fazzini, P. HoloJ: Software suite for holographic reconstruction. http://webarch.bo.imm.cnr.it/ortolani/HoloJ (accessed 2009).
[8] Volkl E., Allard L., Joy D. (Editors), Introduction to electron holography, Kluver Academic Press, New York, 999.
[9] Zhang X., Kuo J., Gu M., Fan X., Bai P., Song Q., Sun C. Local structure relaxation, quantum trap depression, and valence charge polarization induced by the shorter-and-stronger bonds between under-coordinated atoms in gold nanostructures. Nanoscale 2010; 2:412-417.
[10] Sun C., Bai H.L., Tay B.K., Li S. Jiang E.Y. Dimension, strength, and chemical and thermal stability of a single C-C bond in carbon nanotubes. J. Phys. Chem. B 2003;107:7544-7546
[11] Schowalter M., Titantah J.T., Lamoen D., Kruse P. Ab initio computation of the mean inner Coulomb potential of amorphous carbon structures. Appl. Phys. Lett. 2005;86:112102.